Geometrical and Linkage Isomers of $[OsCl_2(dmso)_4]$ − The Complete Picture

Enzo Alessio,*[a] Barbara Serli,[a] Ennio Zangrando,[a] Mario Calligaris,[a] and Natalia S. Panina[b][‡]

Keywords: Density functional calculations / Dimethyl sulfoxide / Isomerizations / Osmium

The isomerisation between the three known isomers of the $[OsCl_2(dmso)_4]$ complex — *trans*-$[OsCl_2(dmso\text{-}S)_4]$ (**1**), *cis,fac*-$[OsCl_2(dmso\text{-}S)_3(dmso\text{-}O)]$ (**2**), and *cis*-$[OsCl_2(dmso\text{-}S)_4]$ (**3**) — has been investigated by NMR spectroscopy, X-ray crystallographic analysis, and DFT calculations. We show that the two dmso-linkage isomers **2** and **3** equilibrate slowly at room temperature in solutions of both dimethyl sulfoxide (DMSO) and light-protected chloroform. Although crystals of **2** precipitate from DMSO solutions, crystals of **3** were obtained from chloroform solutions. Compound **2** isomerises to **1** after exposure to sunlight, while **1** transforms into **2** in hot DMSO solution. The molecular energies were calculated by DFT methods, which show that in the gas phase there are small differences in the total energies (E_t), with **1** exhibiting the lowest energy, in contrast with its low population in solution. This result indicates that the stability of each isomer in solution is not simply determined by E_t, but that the solvent plays an important role. In fact, quantum chemical calculations for the isomerisation process **1** → **2** show a marked increase in the equilibrium constant with increasing the solvent polarity. The calculation of the metal–dmso binding energies, in combination with the X-ray data, shows a significantly higher strength of Os–S bonds with respect to Ru–S bonds, which explains the different behaviour of otherwise analogous osmium–dmso and ruthenium–dmso complexes.

Introduction

Neutral ruthenium(II) halide dimethyl sulfoxide complexes are widely used precursors in inorganic synthesis.[1] In addition, these complexes have anti-tumour[2] and radiosensitising[3] properties, as well as catalytic activity.[4]

Dimethyl sulfoxide (dmso) is an ambidentate ligand that can bind to metal centres either through the sulfur (dmso-*S*) or through the oxygen atom (dmso-*O*). The binding mode of dmso at the RuX_2 centre (X = Cl, Br) has been a matter of interest and debate since the characterisation of *cis,fac*-$[RuX_2(dmso\text{-}S)_3(dmso\text{-}O)]$ and the corresponding thermodynamically less stable geometrical/linkage isomers, *trans*-$[RuX_2(dmso\text{-}S)_4]$.[5−7] The structural and spectroscopic data for these four neutral species, together with those concerning the dinuclear compound $[Ru_2Cl_4(dmso\text{-}S)_5]$,[8] and the charged species [Y][*fac*-$RuCl_3(dmso\text{-}S)_3$] (Y = NH_2Me_2 or RR′NHOH),[9] [*fac*-$RuCl(dmso\text{-}O)_2(dmso\text{-}S)_3][BF_4]$,[10] and [*fac*-$Ru(dmso\text{-}O)_3(dmso\text{-}S)_3][BF_4]_2$,[10,11] have suggested that dmso prefers to bind to Ru^{II} through the sulfur atom for electronic reasons, and that the facial geometry of three dmso-*S* ligands seems to be a particularly stable binding motif. However, coordination of dmso through the sulfur atom is sterically more demanding, compared to coordination through the oxygen atom, and apparently the *fac*-$[Ru(dmso\text{-}S)_3]$ fragment allows coordination of further dmso ligands only through their oxygen atoms for steric reasons.[12] We have also shown that replacement of one dmso-*S* unit by a strongly π-accepting ligand, such as CO or NO, induces the S-to-O-linkage isomerisation of one or more of the remaining dmso units.[13,14] This behaviour was expected since dmso-*S* is a moderate π-acceptor ligand and, thus, it binds preferentially *trans* to pure σ donor ligands; when strong π-acceptors are present in the metal coordination sphere, dmso prefers to bind through its oxygen atom to avoid competition for π electrons.

The synthesis of *cis,fac*-$[OsCl_2(dmso\text{-}S)_3(dmso\text{-}O)]$ and of *trans*-$[OsCl_2(dmso\text{-}S)_4]$,[15] together with the X-ray crystallographic characterisation of *trans*-$[OsBr_2(dmso\text{-}S)_4]$,[16] were in perfect agreement with the previous reports on the analogous ruthenium species and suggested that Os^{II} behaves essentially as does Ru^{II}. This seemingly well-defined belief was shaken, however, in 1998 by McDonagh et al. who reported the X-ray structural characterisation of the unprecedented all-S-bonded isomer *cis*-$[OsCl_2(dmso\text{-}S)_4]$,[17] which showed that the two metal ions can behave quite differently.

[a] Dipartimento di Scienze Chimiche, Università di Trieste
Via L. Giorgieri 1, 34127 Trieste, Italy
Fax: (internat.) + 39-040/558-3903
E-mail: alessi@univ.trieste.it
[b] St. Petersburg State Technological Institute (Technical University),
Moscovsky Prospect 26, St. Petersburg 198013, Russia
[‡] Author to be addressed about quantum chemical calculations.

  DOI: 10.1002/ejic.200300132

Here we report the results of a combined structural, spectroscopic and computational investigation of the three $[OsCl_2(dmso)_4]$ isomers that we undertook with the aim of gaining a better understanding of the system.

Results and Discussion

Solution Behaviour

The complex *trans*-$[OsCl_2(dmso\text{-}S)_4]$ (**1**) was prepared, as described by Antonov et al.,[15] by treatment of $H_2[OsCl_6]$ with $SnCl_2$ in DMSO at 100 °C (Scheme 1); complex **1** spontaneously precipitates from the hot reaction mixture. This compound was structurally and spectroscopically characterised by McDonagh et al.[17] We found, by NMR spectroscopy, that this isomer is quite stable in $CDCl_3$ solution at ambient temperature: the intensity of the resonance at $\delta = 3.44$ ppm, which accounts for the four equivalent dmso-S ligands, decreased very slowly over a period of days and the signal for free DMSO at $\delta = 2.62$ ppm increased correspondingly. No new resonance for coordinated dmso appeared as a consequence of dmso-*S* hydrolysis from **1**. A similar behaviour was found also in D_2O ($\delta = 3.47$ ppm for dmso-*S*). In contrast, the corresponding Ru^{II} isomer, which presumably binds dmso-*S* more weakly (see below), releases one dmso unit immediately upon dissolution in $CDCl_3$ and two *cis* dmso units upon dissolution in D_2O.[7a]

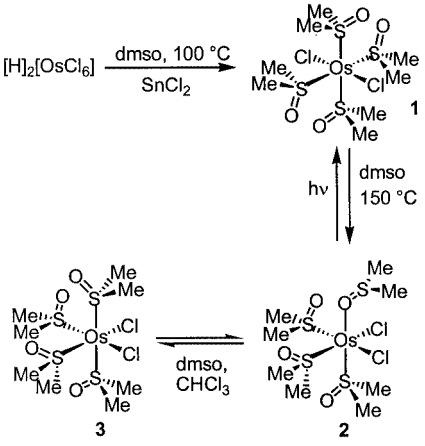

Scheme 1

As described by Antonov et al.,[15] when the above reaction was performed at higher temperature (150 °C), complete dissolution of the *trans* isomer **1** occurred and a white precipitate (**2**) formed from the DMSO solution after cooling to room temperature and addition of acetone (Scheme 1). The spectroscopic signature of this compound,[15] reported also by McDonagh et al.,[17] is typical of *cis*,*fac*-$[OsCl_2(dmso\text{-}S)_3(dmso\text{-}O)]$ (**2**); the presence of O-bonded dmso in **2** was established unequivocally by both NMR and IR spectroscopy. We monitored the isomerisation from **1** to **2** in hot DMSO by visible spectroscopy: at 90 °C the absorption band at 360 nm of the yellow isomer *trans*-$[OsCl_2(dmso\text{-}S)_4]$ (**1**) is completely replaced by that of the colourless *cis* isomer **2** (absorption maximum at 294 nm) within 8 h, with a clear isosbestic point at 282 nm. Recrystallisation of **2** from hot DMSO, followed by addition of acetone, yielded crystals of the same isomer, whose structure was determined by X-ray crystallography (see below). However, as described by McDonagh et al.,[17] crystallisation of **2** at room temperature from chloroform/diethyl ether mixtures yielded crystals that were found by X-ray crystallography to correspond to the all-S-bonded isomer, *cis*-$[OsCl_2(dmso\text{-}S)_4]$ (**3**). Thus, an isomerisation from **2** to **3** must occur in the chloroform solution, while this transformation was not observed in a DMSO solution (Scheme 1).

We found that two sets of resonances are present initially in the ^1H NMR spectrum of **2** in $CDCl_3$ (crystals from the batch used for the X-ray analysis): the major set contains four singlets of equal intensity and corresponds to **2** (dmso-*S* at $\delta = 3.57$, 3.54, and 3.43 ppm; dmso-*O* at $\delta = 2.76$ ppm), while the minor set contains only two equally intense singlets in the region of S-bonded dmso ($\delta = 3.66$ and 3.50 ppm) and corresponds to **3**. The signals of **2** are gradually replaced by those of **3**; equilibrium between the two isomers is reached after ca. 8 d at room temperature (light-protected solution); for longer observation periods (16 d) a very small signal for **1** was also apparent. The equilibrium concentrations of the three isomers correspond to ca. 66% of **3**, 33% of **2**, and less than 1% of **1**. The isomerisation is accompanied by partial hydrolysis of dmso (at equilibrium free DMSO accounts for 5% of the total DMSO) and by the growth of a new minor singlet in the region of S-bonded dmso at $\delta = 3.56$ ppm, which was not assigned. These results confirm the observations of McDonagh et al.[17] A similar behaviour was found to occur also in deuterated DMSO solution ($\delta = 3.41$, 3.38, 3.25, and 2.74 ppm for **2**; $\delta = 3.56$ and 3.40 ppm for **3**); in this case, however, the isomerisation of **2** into **3** could not be followed over a long period of time because of the concomitant exchange of coordinated dmso with the deuterated solvent that led to gradual disappearance of the signals. Thus, in both chloroform and DMSO solution, *cis*,*fac*-$[OsCl_2(dmso\text{-}S)_3(dmso\text{-}O)]$ (**2**) appears to be slightly thermodynamically less stable than *cis*-$[OsCl_2(dmso\text{-}S)_4]$ (**3**) and an equilibrium between the two isomers is established. While crystals of **2** were obtained from DMSO solutions, crystals of **3** were obtained from chloroform solutions.

Finally, as in the case of the corresponding Ru^{II} compounds,[7a] we found that exposure of **2** in solution to sunlight led to its isomerisation to the *trans* isomer **1**. This process was followed by visible spectroscopy in DMSO solution and by NMR spectroscopy in $CDCl_3$ solution.

X-ray Crystal Structure of *cis*,*fac*-$[OsCl_2(dmso\text{-}S)_3(dmso\text{-}O)]$ (2)

The results of the crystal structure determination show that *cis*,*fac*-$[OsCl_2(dmso\text{-}S)_3(dmso\text{-}O)]$ (**2**) (Figure 1) is isostructural with one of the three polymorphs (**F3**) isolated for the ruthenium analogue, *cis*,*fac*-$[RuCl_2(dmso\text{-}S)_3(dmso\text{-}O)]$.[7a] The molecular geometry of this form differs from that detected in its other monoclinic (**F1**)[5] and orthorhom-

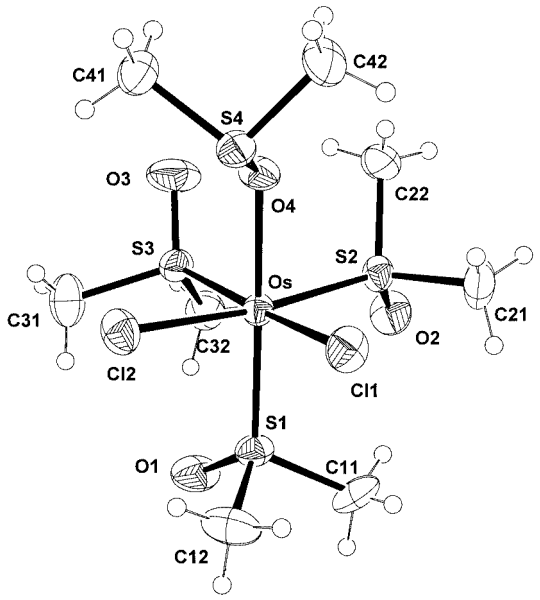

Figure 1. Molecular structure of the compound *cis,fac*-[$OsCl_2$(dmso-*S*)$_3$(dmso-*O*)] (**2**) (thermal ellipsoids drawn at a 40% probability level) with atom numbering scheme

bic (**F2**)[18] crystals, essentially by the different conformation assumed by the dmso-*S* groups upon rotation about the Ru−S bonds.[7a] Infrared spectra have shown that **F2** is the thermodynamically less stable rotamer, which transforms slowly in the solid state into **F3**, in agreement with Molecular Mechanics calculations suggesting that **F3** has the lowest molecular strain energy.[9b] The minimum-strain-energy structure is characterised by a skewed arrangement of the O and S planes of the three dmso-*S* groups (dihedral angle, $\alpha = 25.8°$) and by a *trans*−*trans* conformation of the dmso-*O* group (torsion angle Ru−O−S−C, ψ_1, in the range $-167° < \psi_1 < -90°$).[19] Owing to the similarities between the Os and Ru complexes, the experimental values of $\alpha = 24.2°$ and $\psi_1 = -121.5°$ in the osmium complex **2** suggest that the present molecular structure, found in the solid state, corresponds to the most stable rotamer for this isomer.

Comparison of the Os−S bond lengths in **2** (Table 1) with those of its isomers, *trans*-[$OsCl_2$(dmso-*S*)$_4$] (**1**) (Table 2)[20] and *cis*-[$OsCl_2$(dmso-*S*)$_4$] (**3**) (Table 3),[17] shows a lengthening of the Os−S bond lengths *trans* to S, with respect to those *trans* to Cl or O, as generally observed in metal (e.g., Ru, Rh, Pd, and Pt) sulfoxide complexes.[12,21] However, in **3** the Os−S distances, *trans* to S, are ca. 0.014 Å longer than those in **1**, probably because of stronger steric interactions. The steric demand of the four dmso-*S* groups in **3** is also indicated by the fact that the axial *trans* dmso-*S* groups are pushed away from the *cis* dmso-*S* groups, towards the less-bulky chloride ligands [av. S−Os−S angle, 93(2)°; av. Cl−Os−S angle, 87(2)°]. Similarly, in the equatorial plane, the S−Os−S and Cl−Os−Cl bond angles are 91.60(4)° and 85.42(4)°, respectively. In **1**, the bond angles between the *cis* ligands are restricted to 90°, with the four dmso-*S* groups strictly "interlocked", so that their oxygen atoms lie between the two methyl groups of the adjacent ligand. This arrangement suggests a marked reduction in flexibility on going from **2** and **3** to **1**. The greatest flexibility is to be expected in **2**, because the S→O isomerisation of one of the two *trans* dmso groups leads to a greater degree of rotational freedom.[22]

Finally, the Os−Cl and Os−O bond lengths in **2** are ca. 0.010 and 0.025 Å longer , respectively, than the corresponding distances in the Ru derivative, which is in agreement with the slightly larger covalent radius for the osmium atom. In contrast, we note that the Os−S distances are ca. 0.008 Å shorter than the corresponding Ru−S distances,

Table 1. Observed and calculated selected bond lengths [Å] and angles [°] for *cis,fac*-[$OsCl_2$(dmso-*S*)$_3$(dmso-*O*)] (**2**)

Distance	Exp.	Calcd.
Os−Cl1	2.434(2)	2.473
Os−Cl2	2.428(2)	2.475
Os−S1	2.246(2)	2.300
Os−S2	2.263(2)	2.306
Os−S3	2.277(2)	2.346
Os−O4	2.159(5)	2.168
S1−O1	1.475(6)	1.508
S3−O2	1.472(7)	1.511
S2−O3	1.451(7)	1.507
S4−O4	1.539(6)	1.568
Angle	**Exp.**	**Calcd.**
Cl1−Os−Cl2	87.25(8)	87.89
Cl1−Os−S1	90.52(8)	91.32
Cl1−Os−S2	91.98(8)	91.17
Cl1−Os−S3	173.93(8)	173.93
Cl1−Os−O4	86.0(2)	84.67
Cl2−Os−S1	90.13(9)	89.98
Cl2−Os−S2	172.75(8)	172.41
Cl2−Os−S3	89.32(8)	89.47
Cl2−Os−O4	86.4(2)	86.01
S1−Os−S2	97.09(8)	97.58
S1−Os−S3	94.50(8)	94.14
S1−Os−O4	175.2(2)	174.42
S2−Os−S3	90.79(8)	90.73
S2−Os−O4	86.4(2)	86.40
S3−Os−O4	88.8(2)	89.70

Table 2. Observed and calculated selected bond lengths [Å] and angles [°] for *trans*-[$OsCl_2$(dmso-*S*)$_4$] (**1**)

Distance	Exp.[a]	Calcd.
Os−Cl	2.415(1)	2.479
Os−S	2.3379(9)	2.396
S−O	1.485(4)	1.513
Angle	**Exp.[a][b]**	**Calcd.**
Cl−Os−Cl	180.0	180.00
Cl−Os−S	90.0	90.00
S−Os−S[c]	90.0	90.00
S−Os−S[d]	180.0	180.00

[a] From ref.[20] [b] Symmetry fixed. [c] In *cis* positions. [d] In *trans* positions.

Table 3. Observed and calculated selected bond lengths [Å] and angles [°] for *cis*-$[OsCl_2(dmso\text{-}S)_4]$ (**3**)

Distance	Exp.[a]	Calcd.
Os−Cl1	2.424(1)	2.483
Os−Cl2	2.427(1)	2.484
Os−S1	2.349(1)	2.405
Os−S2	2.275(1)	2.350
Os−S3	2.277(1)	2.350
Os−S4	2.355(1)	2.405
S1−O1	1.474(3)	1.508
S2−O2	1.483(3)	1.511
S3−O3	1.479(3)	1.511
S4−O4	1.467(4)	1.508
Angle	**Exp.[a]**	**Calcd.**
Cl1−Os−Cl2	85.42(4)	89.56
Cl1−Os−S1	89.42(4)	86.76
Cl1−Os−S2	91.39(4)	90.00
Cl1−Os−S3	176.99(4)	177.43
Cl1−Os−S4	85.03(4)	84.95
Cl2−Os−S1	84.75(4)	84.93
Cl2−Os−S2	176.74(4)	177.42
Cl2−Os−S3	91.60(4)	90.05
Cl2−Os−S4	88.80(5)	86.71
S1−Os−S2	94.58(4)	95.79
S1−Os−S3	90.70(4)	92.50
S1−Os−S4	171.81(4)	168.26
S2−Os−S3	91.60(4)	90.51
S2−Os−S4	91.58(4)	92.50
S3−Os−S4	94.54(4)	95.73

[a] The numbering scheme for **3** and the experimental bond lengths and angles are from ref.[17]

suggesting a strengthening of the metal-to-sulfur bonds in the osmium(II) complexes.

Gas-Phase Structures of the $[OsCl_2(dmso)_4]$ Isomers 1−3

Selected bond lengths and angles calculated for the three isomers **1**, **2**, and **3** are reported in Tables 1−3, respectively, together with the experimental values. Inspection of the tables shows a good agreement between experimental and calculated bond lengths, making allowance for an average systematic 2.3% overestimate of the calculated bond lengths. On the other hand, bond angles show both positive and negative deviations, with an average difference of −0.07°.

The calculated Mulliken atomic charges in the isomers of $[OsCl_2(dmso\text{-}S)_4]$ (Table 4) show that the highest dmso-to-O electron density transfers take place for the isomers with all-S-coordinated dmso ligands, **1** and **3**. In accordance with these effects, we observe the lowest electronic energy contribution (E_e, Table 5) to the total molecular energy (E_t) for **1** and **3**. Interestingly, for the isomer **3**, *cis*-$[OsCl_2(dmso\text{-}S)_4]$, we found the highest nuclear repulsion energy contributions (E_n), which likely reflects the steric repulsion effects.

Table 5. Total molecular energy (E_t) with its electronic (E_e) and nuclear repulsion (E_n) energy components for the three isomers of $[OsCl_2(dmso)_4]$, scaled with respect to isomer **1**

Isomer	E_e (a.u.)	E_n (a.u.)	E_t (a.u.)
1 *trans*-$[OsCl_2(dmso\text{-}S)_4]$	0.00000	0.00000	0.00000
2 *cis*-$[OsCl_2(dmso\text{-}S)_3(dmso\text{-}O)]$	40.66623	−40.65683	0.00940
3 *cis*-$[OsCl_2(dmso\text{-}S)_4]$	−14.07069	14.07620	0.00551

Molecular Energies and Isomer Equilibration

The calculated molecular energies of 0.0, 24.7, and 14.4 kJ·mol^{-1}, for **1**, **2**, and **3**, respectively (Table 6), show that in the gas phase the isomer **1**, *trans*-$[OsCl_2(dmso\text{-}S)_4]$, exhibits the lowest energy. The molecular energy differences [$\Delta E_1 = E(\mathbf{2}) - E(\mathbf{1}) = 24.7$ kJ·mol^{-1}, $\Delta E_2 = E(\mathbf{3}) - E(\mathbf{2}) = -10.3$ kJ·mol^{-1}, $\Delta E_3 = E(\mathbf{3}) - E(\mathbf{1}) = 14.4$ kJ·mol^{-1}] are relatively small, yet they are indicative of a preference, in the isolated molecules, for all-S-bonded arrangements (**1** and **3**). On the other hand, a comparison with the experimental population ratios (**1/2/3** = 1:33:66) suggests that, in solution, solvent interactions lower the molecular energies of **2** and **3** with respect to **1**. In fact, the calculated values of ΔE_1 and ΔE_3 in $CHCl_3$ solution are 0.7 and 5.1 kJ·mol^{-1}, respectively, and −9.8 and 0.8 kJ·mol^{-1}, respectively, in DMSO (Table 7). Interestingly, the stabilisation of **2** and **3** relative to **1** increases with the increase in solvent polarity (from $CHCl_3$ to DMSO), paralleling the increase of the solvation energy, E_s (Table 7). The effect is particularly evident for **2**. We have to consider, however, that the equilibrium constant (K) between each pair of isomers is related to its free energy difference, according to the relationship $\ln K = -\Delta G/RT$, with $\Delta G = \Delta H - T\cdot\Delta S$. The term ΔE is only a part of ΔH, as shown by the equation $\Delta H = \Delta E + \Delta ZPE + \Delta H' + R\cdot T$, where ΔZPE is the difference in the zero-point vibration energy, and $\Delta H' = \Delta E_{vib} + \Delta E_{rot} + \Delta E_{trans}$ is the difference between the sums of the vibration, free rotation and translation energy contributions. In the present case, these additional terms can play an important role because of the small ΔE values. The values of ΔZPE, $\Delta H'$, and ΔS were calculated from the normal mode frequencies of the compounds, in the gas phase, on the basis

Table 4. Mulliken atomic electron charges, q [e], in the three isomers of $[OsCl_2(dmso)_4]$

Isomer	$q(Cl_1)$	$q(Cl_2)$	q(dmso-S_1)	q(dmso-S_2)	q(dmso-S_3)	q(dmso) [a]	q(Os)
1	−0.45	−0.45	0.45	0.45	0.45	0.45 ($-S_4$)	−0.90
2	−0.44	−0.44	0.30	0.39	0.39	0.24 (−O)	−0.44
3	−0.43	−0.43	0.47	0.40	0.40	0.47 ($-S_4$)	−0.88

[a] Coordinated atom in parentheses.

of the DFT force field. From the data in Table 6 we obtained, for the isomerisation process **1** → **2**, ΔZPE = −7.6 kJ·mol^{-1}, $\Delta H'$ = 3.1 kJ·mol^{-1}, and ΔS = 35.3 J·mol^{-1}·K^{-1}, so that ΔG(298 K) = 9.7 kJ·mol^{-1} and K = 2.0·10^{-2}. For the isomerisation process **2** → **3**: ΔZPE = 7.3 kJ·mol^{-1}, $\Delta H'$ = −3.5 kJ·mol^{-1}, ΔS = −33.3 J·mol^{-1}·K^{-1}, ΔG(298 K) = 3.4 kJ·mol^{-1}, K = 2.5·10^{-1}; for the isomerisation process **1** → **3**: ΔZPE = −0.3 kJ·mol^{-1}, $\Delta H'$ = −0.4 kJ·mol^{-1}, ΔS = 2.0 J·mol^{-1}·K^{-1}, ΔG(298 K) = 13.1 kJ·mol^{-1}, K = 5.0·10^{-3}. The trend in the values of ΔS is consistent with that expected from the variation of the conformational entropy of each isomer pair. The highest value is calculated for the process **1** → **2**. In fact, in **2** there is the maximum degree of rotational freedom, while in **1** this rotation is strongly restricted because the four dmso-*S* groups are "blocked' in the equatorial plane (see the X-ray structure section above).

Table 6. Total molecular energy, E_t (kJ·mol^{-1}), in the gas phase, for the three isomers of [$OsCl_2$(dmso)$_4$], scaled with respect to isomer **1**. The zero-point vibration energy (ZPE, kJ·mol^{-1}), the sum of the vibration, free rotation, and translation energy contributions (H', kJ·mol^{-1}), and the entropy value (S, J·mol^{-1}), are also reported

Isomer		E_t (gas)	ZPE	H'	S
1	*trans*-$OsCl_2$(dmso-*S*)$_4$	0.0	877.0	77.6	731.8
2	*cis*-$OsCl_2$(dmso-*S*)$_3$(dmso-*O*)	24.7	869.4	80.7	767.1
3	*cis*-$OsCl_2$(dmso-*S*)$_4$	14.4	876.7	77.2	733.8

The above calculated equilibrium constants, however, which show a prevalence of isomer **1**, are not consistent with the experimental data (**1**/**2**/**3** = 1:33:66). Accounting for the solvation energy, E_s($CHCl_3$) (Table 7), in the calculations for the process **1** → **2**, leads to a lower value of ΔG(298 K) (−14.3 kJ·mol^{-1}), and a corresponding increase in the equilibrium constant to 3.2·10^2. In DMSO solution, because of the greater solvation energy, E_s(dmso) (Table 7), ΔG(298 K) = −24.8 kJ·mol^{-1}, with a further increase of the equilibrium constant (K = 2.2·10^4). For the process **2** → **3**, the corresponding values are ΔG(298 K) = 18.1 kJ·mol^{-1} and K = 6.6·10^{-4} in $CHCl_3$; in DMSO, ΔG(298 K) = 24.3 kJ·mol^{-1} and K = 5.4·10^{-5}. Thus, the calculations show that formation of isomers **2** and **3** is largely preferred, in chloroform and DMSO solutions, with respect to that of **1**. Complex **2** should prevail over **3**, however, for both entropy and solvent effects. In fact, to evaluate the equilibrium constants correctly, the terms ΔZPE, $\Delta H'$, and ΔS should be derived from the normal mode frequencies of the compounds calculated in solution, rather than in gas phase, which is a calculation that is somewhat problematic at present.

The different behaviour of the ruthenium analogue of **2**, *cis*-[$RuCl_2$(dmso-*S*)$_3$(dmso-*O*)], which does not isomerise to *cis*-[$RuCl_2$(dmso-*S*)$_4$], is likely related to the weaker metal−S bonds in the Ru complexes. In fact, the Os−S bond lengths are, on average, ca. 0.008 Å shorter than the corresponding Ru−S bond lengths. Furthermore, previous DFT calculations have shown that *cis*-[$RuCl_2$(dmso-*S*)$_4$] exhibits a molecular energy that is 56 kJ·mol^{-1} higher than that of *cis*-[$RuCl_2$(dmso-*S*)$_3$(dmso-*O*)],[24] while our present calculations show that in the corresponding Os derivatives this energy is 10.3 kJ·mol^{-1} lower.

The increased strength of the Os−S bonds relative to the Ru−S bonds, which is suggested by the trend of the bond lengths, is supported by the DFT calculations of the M−dmso binding energies, BE,[23] in the *cis*-MCl_2(dmso-*S*)$_3$(dmso-*O*) complexes, M = Ru and Os (Table 8). We note that all of the binding energies are higher in the Os derivative, but the energy differences are significantly larger for the M−S bonds [BE^S(Os) − BE^S(Ru) = 32.2 and 40.7 kJ·mol^{-1}, for dmso-*S*-*trans*-to-Cl and dmso-*S*-*trans*-to-O, respectively) than for the M−O bonds [BE^O(Os) − BE^O(Ru) = 11.6 kJ·mol^{-1}, for dmso-*O*-trans-to-S). Interestingly, in both the Ru and Os complexes, BE^S(dmso-*S*-*trans*-to-O) is larger than BE^S(dmso-*S*-*trans*-to-Cl), in agreement with the observed M−S1 distances (Os, 2.246 Å; Ru,[7a] 2.245 Å), which are significantly shorter than values of M−S2 and M−S3 (Figure 1) (Os, av. 2.270 Å; Ru,[7a] av. 2.279 Å).

Table 8. M−dmso binding energies, BE (kJ·mol^{-1}), for *cis*-[MCl_2(dmso-*S*)$_3$(dmso-*O*)]

M	dmso-*S* (*trans*-Cl)	dmso-*S* (*trans*-*O*)	dmso-*O* (*trans*-*S*)
Os	166.8	213.4	137.1
Ru	134.6	172.7	125.5

Conclusions

We have shown by NMR spectroscopy that at room temperature, both in light-protected $CDCl_3$ and [D_6]DMSO solutions, *cis*,*fac*-[$OsCl_2$(dmso-*S*)$_3$(dmso-O)] (**2**) equilibrates slowly with its linkage isomer, *cis*-[$OsCl_2$(dmso-*S*)$_4$] (**3**). For very long observation times in chloroform solution (16 d),

Table 7. Total molecular energy, E_t (kJ·mol^{-1}), in gas phase and in chloroform and DMSO solutions, for the three isomers of [$OsCl_2$(dmso)$_4$], scaled with respect to isomer **1**. The solvation energies of $CHCl_3$ and DMSO, E_s (kJ·mol^{-1}), are also reported

Isomer		E_t (gas)	E_t ($CHCl_3$)	E_s ($CHCl_3$)	E_t (DMSO)	E_s (DMSO)
1	*trans*-[$OsCl_2$(dmso-*S*)$_4$]	0.0	0.0	−63.6	0.0	−68.7
2	*cis*-[$OsCl_2$(dmso-*S*)$_3$(dmso-*O*)]	24.7	0.7	−87.6	−9.8	−103.2
3	*cis*-[$OsCl_2$(dmso-*S*)$_4$]	14.4	5.1	−72.9	0.8	−82.3

a small amount of *trans*-$[OsCl_2(dmso\text{-}S)_4]$ (**1**) is also formed, with the equilibrium population ratio of **1/2/3** = 1:33:66. Crystals of **2** were obtained from DMSO solutions, while crystals of **3** were obtained from chloroform solutions, most likely because of solubility effects. As previously found for the well-known ruthenium analogues, **2** isomerises to **1** upon exposure of its solution to sunlight. On the other hand, the ruthenium analogue of **3** has never been observed. We attribute such behaviour to the greater preference of osmium(II) for S-bonding, as shown by the trend of the metal−sulfur bond lengths and the calculated metal−dmso binding energies. The molecular energies, calculated in gas phase by the DFT B3LYP method, show small differences between the three osmium isomers, with the lowest energy being exhibited by **1**, whereas, in solution, this isomer is only a minor product. Quantum chemical calculations show that the solvent plays an important role in determining the isomer stability in solution, together with conformational entropy effects. In fact, when taking into account both of these factors, the populations of **2** and **3** largely exceed that of **1**. A quantitative analysis of the isomer distribution is limited by the possibility of calculating the normal mode frequencies only in the gas phase.

Table 9. Crystal and refinement data for *cis*,*fac*-$[OsCl_2(dmso\text{-}S)_3(dmso\text{-}O)]$ (**2**)

Empirical formula	$C_8H_{24}Cl_2O_4OsS_4$
Formula mass	573.61
Cryst system	monoclinic
Space group	$P\ 2_1/n$ (No. 14)
a, Å	8.430(2)
b, Å	27.769(4)
c, Å	8.599(2)
β, deg	116.61(2)
V, Å^3	1799.7(5)
$D_{calcd.}$, g cm^{-3}	2.117
Z	4
μ (Mo-$K\alpha$), mm^{-1}	7.850
$F(000)$	1112
θ range, deg	2.80−27.10
No. of reflns. collcd.	5584
No. of indep. reflns.	3679
R_{int}	0.0536
No. of refined params.	176
goodness-of-fit (F^2)	1.029
$R1$ [$I > 2\sigma(I)$][a]	0.0577
$wR2$ [a]	0.1418
residuals, e/Å^3	2.764[b], −1.283

[a] $R1 = \Sigma||F_o| - |F_c||/\Sigma|F_o|$; $wR2 = [\Sigma w(F_o^2 - F_c^{2)2}/\Sigma w(F_o^2)^2]^{1/2}$. [b] Close to the Os atom.

Experimental Section

The complexes *trans*-$[OsCl_2(dmso\text{-}S)_4]$ (**1**) and *cis*,*fac*-$[OsCl_2(dmso\text{-}S)_3(dmso\text{-}O)]$ (**2**) were prepared as described by Antonov et al.[15]

Materials: Chemicals, including $H_2OsCl_6{\cdot}6H_2O$ and deuterated solvents, were purchased from Aldrich and used as received. Electronic absorption spectra were recorded in quartz cells with a Jasco UV/Vis V500 spectrophotometer equipped with a Peltier thermostatic unit. Infrared spectra (KBr) were obtained on a Perkin−Elmer 2000 NIR FT-Raman spectrometer. ^1H and $^{13}C\{^1H\}$ NMR spectra were collected at room temperature at 400 and 100.5 MHz, respectively, on a Jeol Eclipse 400 FT spectrometer, with 2,2-dimethyl-2,2-silapentane-5-sulfonate (DSS) as an internal standard for D_2O solutions and the residual non-deuterated solvent signals as references for spectra in $[D_6]$DMSO (δ = 2.50 ppm) and $CDCl_3$ (δ = 7.26 ppm).

Crystallography: Data collection was carried out on a Nonius DIP-1030H system, equipped with graphite monochromator and Mo-K_α radiation (λ = 0.71073 Å). A total of 30 frames were collected, each with a rotation of 6° about , exposure time of 20 min, detector positioned at 80 mm from the crystal. Cell refinement and data reduction were carried out using the programs Mosflm and Scala.[25] The crystals were found to be isomorphous with those of the ruthenium analogue.[7a] The structure was solved, however, by conventional Fourier methods, using SHELXS-97,[26] to avoid any bias toward any of the possible rotational isomers.[7] Anisotropic refinement was carried out by the full-matrix least-squares method based on F^2 using SHELXL-97.[26] All calculations were performed using the WinGX system, Ver 1.64.03.[27] Crystal data and details of the refinement are listed in Table 9. Bond lengths and angles are given in Table 1.

CCDC-205611 contains the supplementary crystallographic data for this paper. These data can be obtained free of charge at www.ccdc.cam.ac.uk/conts/retrieving.html [or from the Cambridge Crystallographic Data Centre, 12, Union Road, Cambridge CB2 1EZ, UK; Fax: (internat.) +44-1223/336-033; E-mail: deposit@ccdc.cam.ac.uk].

DFT Calculations: The calculations of the electronic structures of the osmium complexes were carried out by means of the DFT B3LYP method with a 6-31G(d,p) basis for main group elements, and with the HW effective core potential (ncore = 60) for the Os atom,[28] using the GAMESS-2001 program set.[29] Solvation energies of the compounds in chloroform solutions were calculated on the basis of the polarised continuum model.[30] Starting coordinates for the geometry optimisation were derived from the X-ray structures. The terms Δ*ZPE*, Δ*H′*, and Δ*S*, used to evaluate the values of Δ*G*, were calculated from the normal-mode frequencies of the compounds, in the gas phase, on the basis of the DFT force field.[29]

Atom and dmso-group charges for the three isomers of $OsCl_2(dmso)_4$ are reported in Table 4. The scaled total molecular energies, with their electronic and nuclear repulsion components, are listed in Table 5. The scaled total molecular energies in the gas phase, together with zero-point vibration energies, the sum of the vibration, free rotation, and translation energy contributions, and entropy values, are reported in Table 6. A comparison of the molecular energies, in the gas phase and in chloroform and DMSO solutions, are given in Table 7, together with the $CHCl_3$ and DMSO solvation energies. Table 8 gives the binding energies of dmso to Os and Ru in the *cis*-$[MCl_2(dmso\text{-}S)_3(dmso\text{-}O)]$ complexes.

Acknowledgments

This work has been supported by MIUR (Rome) (PRIN: 2001053898 004) and the Ministry of Education of the Russian Federation (grant E02-5.0-342).

[1] See, for example: [1a] E. Alessio, M. Calligaris, M. Iwamoto, L. G. Marzilli, *Inorg. Chem.* **1996**, *35*, 2538−2545. [1b] T. Tanase, T. Aiko, Y. Yamamoto, *Chem. Commun.* **1996**, 2341−2342. [1c] E. Alessio, M. Macchi, S. L. Heath, L. G. Marzilli, *Inorg. Chem.* **1997**, *36*, 5614−5623. [1d] S. F. Lessing, S. Lotz, H. M. Roos, P. H. van Rooyen, *J. Chem. Soc., Dalton Trans.* **1999**, 1492−1502. [1e] J. J. Rack, H. B. Gray, *Inorg. Chem.* **1999**, *38*, 2−3. [1f] E. Iengo, G. Mestroni, S. Geremia, M. Calligaris, E. Alessio, *J. Chem. Soc., Dalton Trans.* **1999**, 3361−3371. [1g] M. Biagini Cingi, M. Lanfranchi, M. A. Pellinghelli, M. Tegoni, *Eur. J. Inorg. Chem.* **2000**, 703−711. [1h] E. Alessio, E. Iengo, E. Zangrando, S. Geremia, P. A. Marzilli, M. Calligaris, *Eur. J. Inorg. Chem.* **2000**, 2207−2219. [1i] E. Iengo, E. Zangrando, R. Minatel, E. Alessio, *J. Am. Chem. Soc.* **2002**, *124*, 1003−1013 and references therein.

[2] G. Sava, E. Alessio, A. Bergamo, G. Mestroni, in *Topics in Biological Inorganic Chemistry*, Volume 1, "*Metallo-pharmaceuticals*" (Eds.: M. J. Clarke, P. J. Sadler), Springer, Berlin, **1999**, pp. 143−169.

[3] [3a] P. K. L. Chan, B. R. James, D. C. Frost, P. K. H. Chan, H.-L. Hu, K. A. Skov, *Can. J. Chem.* **1989**, *67*, 508−516. [3b] P. K. L. Chan, P. K. H. Chan, D. C. Frost, B. R. James, K. A. Skov, *Can. J. Chem.* **1988**, *66*, 117−122.

[4] [4a] R. S. Srivastava, B. Milani, E. Alessio, G. Mestroni, *Inorg. Chim. Acta* **1992**, *191*, 15−17. [4b] B. R. James, R. S. McMillan, *Can. J. Chem.* **1977**, *55*, 3927−3932. [4c] B. R. James, R. S. McMillan, K. J. Reimer, *J. Mol. Catal.* **1976**, *1*, 439−441. [4d] D. P. Riley, *Inorg. Chem.* **1983**, *22*, 1965−1967.

[5] A. Mercer, J. Trotter, *J. Chem. Soc., Dalton Trans.* **1975**, 2480−2483.

[6] J. D. Oliver, D. P. Riley, *Inorg. Chem.* **1984**, *23*, 156−158.

[7] [7a] E. Alessio, G. Mestroni, G. Nardin, W. M. Attia, M. Calligaris, G. Sava, S. Zorzet, *Inorg. Chem.* **1988**, *27*, 4099−4106. [7b] J. S. Jaswal, S. J. Rettig, B. R. James, *Can. J. Chem.* **1990**, *68*, 1808−1817.

[8] [8a] G. A. Heath, A. J. Lindsay, T. A. Stephenson, *J. Chem. Soc., Dalton Trans.* **1982**, 2429−2432. [8b] M. Calligaris, P. Faleschini, E. Alessio, *Acta Crystallogr., Sect. C* **1993**, *49*, 663−666.

[9] [9a] R. S. McMillan, A. Mercer, B. R. James, J. Trotter, *J. Chem. Soc., Dalton Trans.* **1975**, 1006−1010. [9b] S. Geremia, M. Calligaris, Y. N. Kukushkin, A. V. Zinchenko, V. Yu. Kukushkin, *J. Mol. Struct.* **2000**, *516*, 49−56.

[10] [10a] J. D. Fotheringham, G. A. Heath, A. J. Lindsay, T. A. Stephenson, *J. Chem. Res. (S)* **1986**, 82−83. [10b] J. R. Barnes, R. J. Goodfellow, *J. Chem. Res. (S)* **1979**, 350−351.

[11] A. R. Davies, F. W. B. Einstein, N. P. Farrell, B. R. James, R. S. McMillan, *Inorg. Chem.* **1978**, *17*, 1965−1969.

[12] M. Calligaris, O. Carugo, *Coord. Chem. Rev.* **1996**, *153*, 83−154.

[13] [13a] E. Alessio, M. Bolle, B. Milani, G. Mestroni, P. Faleschini, S. Geremia, M. Calligaris, *Inorg. Chem.* **1995**, *34*, 4716−4721. [13b] E. Alessio, B. Milani, M. Bolle, G. Mestroni, P. Faleschini, F. Todone, S. Geremia, M. Calligaris, *Inorg. Chem.* **1995**, *34*, 4722−4734.

[14] [14a] B. Serli, E. Zangrando, E. Iengo, G. Mestroni, L. Yellowlees, E. Alessio, *Inorg. Chem.* **2002**, *41*, 4033−4043. [14b] B. Serli, E. Zangrando, E. Iengo, E. Alessio, *Inorg. Chim. Acta* **2002**, *339*, 265−272.

[15] P. G. Antonov, Y. N. Kukushkin, V. I. Konnov, Y. P. Kostikov, *Koord. Khim.* **1980**, *6*, 1585−1589.

[16] P. D. Robinson, C. C. Hinckley, A. Ikuo, *Acta Crystallogr., Sect. C* **1989**, *45*, 1079−1080.

[17] A. M. McDonagh, M. G. Humphrey, D. C. R. Hockless, *Aust. J. Chem.* **1998**, *51*, 807−811.

[18] W. M. Attia, M. Calligaris, *Acta Crystallogr., Sect. C* **1987**, *43*, 1426−1427.

[19] S. Geremia, M. Calligaris, *J. Chem. Soc., Dalton Trans.* **1997**, 1541−1547.

[20] M. F. C. Guedes da Silva, A. J. L. Pombeiro, S. Geremia, E. Zangrando, M. Calligaris, A. V. Zinchenko, V. Yu. Kukushkin, *J. Chem. Soc., Dalton Trans.* **2000**, 1363−1371.

[21] M. Calligaris, *Croat. Chem. Acta* **1999**, *72*, 147−169.

[22] M. Calligaris, P. Faleschini, F. Todone, E. Alessio, S. Geremia, *J. Chem. Soc., Dalton Trans.* **1995**, 1653−1661.

[23] N. S. Panina, M. Calligaris, *Inorg. Chim. Acta* **2002**, *334*, 165−171.

[24] M. Stener, M. Calligaris, *J. Mol. Struct. (Theochem)* **2000**, *497*, 91−104.

[25] Collaborative Computational Project, Number 4, *Acta Crystallogr., Sect. D* **1994**, *50*, 760−763.

[26] G. M. Sheldrick, SHELX97, *Programs for Structure Analysis*, University of Göttingen, **1998**.

[27] L. J. Farrugia, *J. Appl. Cryst.* **1999**, *32*, 837−838.

[28] P. J. Hay, W. R. Wadt, *J. Chem. Phys.* **1985**, *82*, 284−298.

[29] M. W. Schmidt, K. K. Baldrige, J. A. Boatz, S. T. Elbert, M. S. Gordon, J. H. Jensen, S. Koseki, N. Matsunaga, K. A. Nguen, S. J. Su, T. L. Windus, M. Dupuis, J. A. Montgomery, *J. Comput. Chem.* **1993**, *14*, 1347−1363.

[30] J. Tomasi, M. Persico, *Chem. Rev.* **1994**, *94*, 2027−2094.

Received March 10, 2003

